Math. Model. Nat. Phenom. 20 (2025) 14
https://doi.org/10.1051/mmnp/2025006

Mathematical Modelling of Natural Phenomena
www.mmnp-journal.org

THE INTERPLAY BETWEEN EVOLUTIONARY AND IMMUNOLOGICAL DYNAMICS REGULATES VIRUS VARIANT EMERGENCE AND COMPETITION

Anass Bouchnita[1,*], Shraddha Ramdas Bandekar[2], Kaiming Bi[2,3], Behzad Djafari Rouhani[1], Spencer J. Fox[4,5] and Juan A. Garcia[1]

Abstract. As viruses like SARS-CoV-2 and pandemic influenza become endemic, their spread is shaped by decreasing population immunity and the emergence of new variants that either spread more easily or bypass existing immunity. Traditional modeling of these dynamics has been challenging due to increased computational demands as the number of strains and immune profiles grow. We introduce a simplified epidemiological model that incorporates viral evolution, immunological and transmission dynamics, as well as variant-specific factors like disease severity. This model, based on the standard SIR framework and using a COVID-19 specific parameters, explores the interaction between immunological and evolutionary mechanisms. It suggests that in the absence of broad cross-immunity, different variants can co-exist together. The model predicts that viruses with higher transmissibility, mutation rates are more likely to evolve, while variants with reduced immune escape have a higher emergence potential. In scenarios where an emerging variant's transmissibility doubles, the model forecasts a sevenfold increase in cases over 2,000 days. While parameterized using COVID-19 data, our model can be adapted for other viruses with evolving strains, such as influenza or Dengue. Hence, it promises to enhance our capacity to predict variant developments and guide public health strategies.

Mathematics Subject Classification. 92-10, 92B05, 45K05.

Received April 17, 2024. Accepted February 3, 2025.

1. Introduction

Virus evolution and variant emergence are critical concerns in public health due to their potential to significantly alter the course of infectious disease outbreaks [1]. As viruses replicate, they can mutate, leading to the creation of new variants that may have different characteristics from the original strain. These new variants can be more transmissible, potentially increasing the speed and reach of an outbreak and placing greater

Keywords and phrases: Immuno-epidemiological modeling, genotype-structured models, epidemiological modeling, reaction-diffusion systems, genetic mutations.

[1] Department of Mathematical Science, The University of Texas at El Paso, El Paso, TX 79968, USA.
[2] Department of Integrative Biology, The Unviersity of Texas at Austin, Austin, TX 78712, USA.
[3] School of Public Health, The University of Texas Health Science Center, Houston, Texas, 77030, USA.
[4] Department of Epidemiology & Biostatistics, University of Georgia, Athens, GA 30602, USA.
[5] Institute of Bioinformatics, University of Georgia , Athens, GA 30602, USA.

* Corresponding author: abouchnita@utep.edu

strain on healthcare systems [2]. They may also be more virulent [3], causing more severe disease and leading to higher rates of hospitalization and mortality. Additionally, existing vaccines and treatments may be less effective against new variants, undermining public health efforts to control the spread of the virus and protect vulnerable populations [4]. Together, these factors underscore the importance of robust surveillance, rapid response, and ongoing research to monitor virus evolution and address the public health challenges posed by emerging variants.

The COVID-19 pandemic has brought to our attention the threat posed by new variants on our public health systems. Throughout the COVID-19 pandemic, the SARS-CoV-2 virus has exhibited a capacity for genetic evolution, resulting in the emergence of multiple variants. Some of these variants have been characterized by enhanced transmissibility, altered virulence, and, critically, varied susceptibility to neutralization by the antibodies generated from prior infection or vaccination. Simultaneously, the natural waning of immune responses over time, post-infection or post-vaccination, has raised concerns about the potential for reinfections and breakthrough cases, especially in the face of these emerging variants [5]. Vaccines, while remarkably successful in reducing severe disease and transmission, can sometimes face challenges in effectively reducing the spread of certain variants. Although they can often still confer protection against severe outcomes in most cases. The interplay between virus evolution and immunological dynamics underscores the dynamic nature of the pandemic and the need for the development of new modeling frameworks which integrate these mechanisms in a flexible way.

COVID-19 is just one of many RNA viruses characterized by the ongoing emergence of variants. Influenza and the human Respiratory Syncytial Virus (RSV) experience alternating seasonal variant emergence. Other rapidly mutating viruses like Hepatitis C Virus (HCV), dengue, Ebola, and Zika have undergone numerous genomic changes since their initial spillover. The mechanisms behind variant emergence are not yet completely understood, but research suggests a combination of factors including high mutation rates, immune response-driven selective pressure [6], recombination events [7], varying population immunity levels [8], and human behavioral influences [9] as key drivers in the evolution and persistence of RNA viruses.

Epidemiological models are vital tools in understanding and predicting the spread of diseases within populations [10]. These models can be broadly categorized into deterministic and stochastic. Deterministic models, like the Susceptible-Infectious-Recovered (SIR) model [5, 11, 12], provide average outcomes and assume fixed parameters, often using differential equations. In contrast, stochastic models account for randomness and uncertainties inherent to disease transmission [13, 14]. They offer a range of possible outcomes depending on the source of the considered uncertainties. Additionally, within these categories, models can be compartmental, where populations are divided into distinct groups like susceptible, exposed or infectious [15], or agent-based [16, 17], where individual entities and their interactions are simulated. Immuno-epidemiological models are another approach which aims to integrate the effect of immunity on the progression of epidemics. Some of these models are multiscale and explicitly integrate within-host infection and between-host transmission models [18–20], while others are continuous and integrate the effect of population immunity into infectious disease dynamics [21–24]. Each type of model offers unique insights, and the choice often depends on the specifics of the disease, available data, and the questions being addressed.

The competition between variants was previously investigated using multi-strain models [25–28]. These models explicitly describe the transmission dynamics of a group of co-circulating strains using a system of equations for each of them. Some of the developed multi-strain models are compatible with phylogenetic data, which increases their ability to predict the competition patterns between virus strains [29]. Their advantage is that they can be analyzed analytically and numerically. However, they require assuming some additional conditions regarding the seeding of new variants, which limits their applicability for studying the dynamics of variant emergence. At the host level, the competition between variants within hosts was also studied using multi-strain models [30]. The integration of epidemiological models with immunodynamics and evolutionary biology has given rise to advanced phylodynamic frameworks [31–33]. These models are suitable for the study of questions related to the analysis of dynamic forces that regulate the emergence and co-circulation patterns observed in RNA viruses. Multi-strain immuno-epidemiological models were also developed to gain insights into the development of multivalent vaccines [34]. Others were combined with phylogenetic and ecological data to investigate the ecological and immunological factors driving influenza evolution [35].

Further, reaction-diffusion equation-based models were developed and analyzed to determine the relationship between viral load and virulence, genotype distribution, and the strength of the immune response [36, 37]. A similar genotype-structured model was developed and analyzed to study the emergence of variants at the population level [38]. This model assumes that the infection rate of variants depends on the strain by which the susceptible individual gets infected and considers that the virus transmissibility changes according to the virus strain. Genotype-structured models were also developed and applied to investigate problems originating from ecology [39], viral infection [40], and tumor growth [41, 42].

To overcome the growing complexity of the immunological and evolutionary landscape of COVID-19, several immuno-epidemiological models were developed [43, 44]. We have previously developed a framework that explicitly tracks population immunity and it's impact on virus suceptbility and virulence [24]. The model describes the growth of different COVID-19 variants using logistic functions fitted to genomic data. It calculates the average susceptibility and severity of the disease based on the history of infections and vaccination. Immune escape is captured by considering that emerging variants reduce the efficacy of prior immunity, while immune waning is modeled by assuming exponential decay of immunity. The model was initially used for making accurate projections of the burden of surges driven by Omicron variants. Then, it was applied to provide timely scenario projections to the COVID-19 and flu Scenario modeling hub [45]. Recently, it was used to provide tripledemic projections which aimed to assess the combined impact of COVID-19, flu and RSV [46], as well as determining equitable vaccination strategies that protect the vulnerable Hispanic population in El Paso County, Texas [47].

In this work, we propose to extend our previously developed immuno-epidemiological modeling approach by incorporating virus evolution and variant emergence [24]. Immuno-epidemiological models incorporating fitness landscapes and evolution were specifically developed for influenza to explore key questions, such as the co-circulation and re-emergence of variants [35, 48]. The model is structured according to the genotype of harbored viruses by infected individuals and a diffusion term is used to capture the changes in the genotype due to virus mutations. The efficacy of population immunity in reducing the transmission and severity of the virus strain depends on the genotypic distance between the harbored antibodies and the circulating strains. We consider fitness landscapes consisting of an original and emerging variant separated by a genotypic distance. We parameterize the model using available literature estimates for COVID-19 transmission and apply it to gain insights into the factors regulating the emergence and competition of variants.

2. Methods and models

2.1. Model description

In this section, we introduce a novel epidemiological model that is structured according to the virus genotype. It captures population immunity through a specific state variable, similar to our previous models for COVID-19, flu and RSV [24]. The model was previously applied to study the co-circulation and competition patterns of influenza variants [49]. We denote the virus genotype by x and consider that it belongs to a one-dimensional genotype space X which characterizes the genetic potential for virus transmission. We assume that the unit considered for the genotype is an arbitrary genetic unit (G.U.). Given the theoretical nature of the study, we consider a bounded genotype space which extends from –2 to 10 G.U. (*i.e.* arbitrary genetic unit). Changes in the virus genotype occur as a result of mutations during virus replication. We model this effect as a diffusion process that describes the changes in the genotype of the virus genotype during infection. The effect of cross-immunity is captured by considering that the efficacy of the generated population immunity depends on the genotypic distance between the strain harbored by infected individuals and antibodies in the population. A schematic representation of the model dynamics is provided in Figure 1, A. To study the emergence of new variants, we consider a function for the infection rate ($\beta(x)$) that reflects a fitness landscape that consists of two variants: (i) variant 0, which represents the original variant that is imported initially into the population and which we consider to be centred at x_0, and (ii) variant X which can potentially emerge during infection and is considered to be centred at x_1. We assume that each of these variants has a radius of 0.5 G.U. In other words, variant 0 extends from $x_0 - 0.5$ to $x_0 + 0.5$, where x_0 is the center of variant 0. We begin with the population

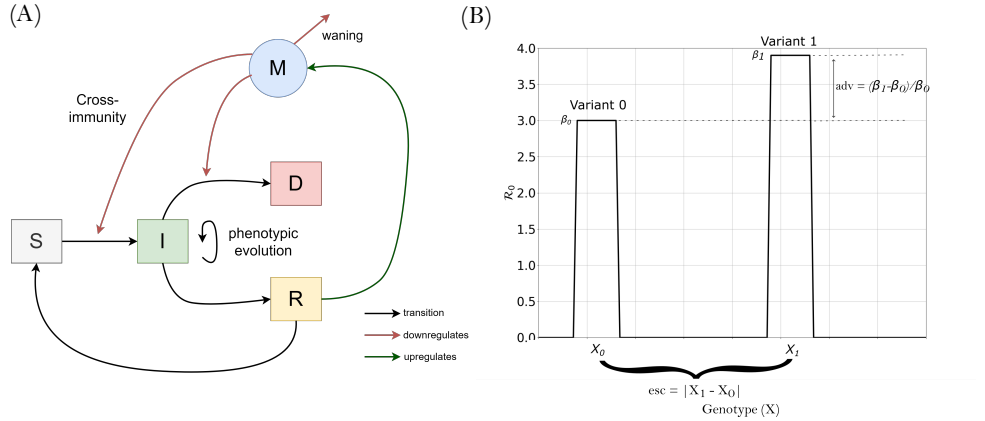

FIGURE 1. (A) The model dynamics are schematically represented, illustrating the progression from the susceptible group (S) to the infected (I), recovered (R), and deceased compartments (D). During infection, individuals in the infected state experience phenotypic alterations resulting from the mutations acquired by the virus during replication. Similar to our previous models [24], individuals in the recovered state rapidly lose immunity, but they contribute to the overall population immunity level, denoted by M. This population immunity level modulates the average susceptibility and disease severity, which varies based on the genotype of circulating strains and the extent of cross-immunity. (B) A representation of the fitness landscape for the basic reproduction number that is considered in the simulations to study variant emergence and competition. It shows two viable spaces corresponding to two variants 0 and 1 separated by a genotypic distance $\Delta x = |x_0 - x_1|$. Variant 1 has a transmissiblity advantage over variant 0, described by assuming an elevated relative infection rate.

of susceptible individuals, which does not depend on the virus genotype:

$$\frac{\mathrm{d}S}{\mathrm{d}t}(t) = -S(t)\int_X \beta(x)\frac{I(x,t)}{1+K_1\int_X \phi_x(y,d_0)M(y,t)\mathrm{d}y}\mathrm{d}x + \delta\int_X R(x,t)\mathrm{d}x. \tag{2.1}$$

Here, the first term on the right-hand side of the equation describes the infection of susceptible individuals, with β denoting the infection rate, K_1 is the efficacy of immunity against susceptibility, and d_0 is the cross-immunity broadness. The second term represents the transition of individuals from a recovered compartment to a susceptible one, which is assumed to occur very fast in the model and whose rate is denoted by δ. Next, we describe the population of infected individuals. These individuals are structured according to the phenotype of the virus that they harbor:

$$\begin{aligned}\frac{\partial I}{\partial t}(x,t) = \theta(t)\Delta I(x,t) + \beta(x)S(t)\frac{I(x,t)}{1+K_1\int_X \phi_x(y,d_0)M(y,t)\mathrm{d}y} - \mu_1 I(x,t)\\ - \mu_2\frac{I(x,t)}{1+K_2\int_X \phi_x(y,d_0)M(y,t)\mathrm{d}y}.\end{aligned} \tag{2.2}$$

Here, the first term on the right hand side of the equation represents the changes in the genotype of infected individuals harboring the virus due to acquired mutations during infection. This change is driven by virus replication during infections. Assuming that each host undergoes a replication of variants during infections, we can model the genotype change in each host as independent diffusion processes. Assume that these diffusion processes are independent of x, we can also describe multiple diffusion processes occurring in multiple hosts at the same time as another diffusion process as shown in Figure 2.

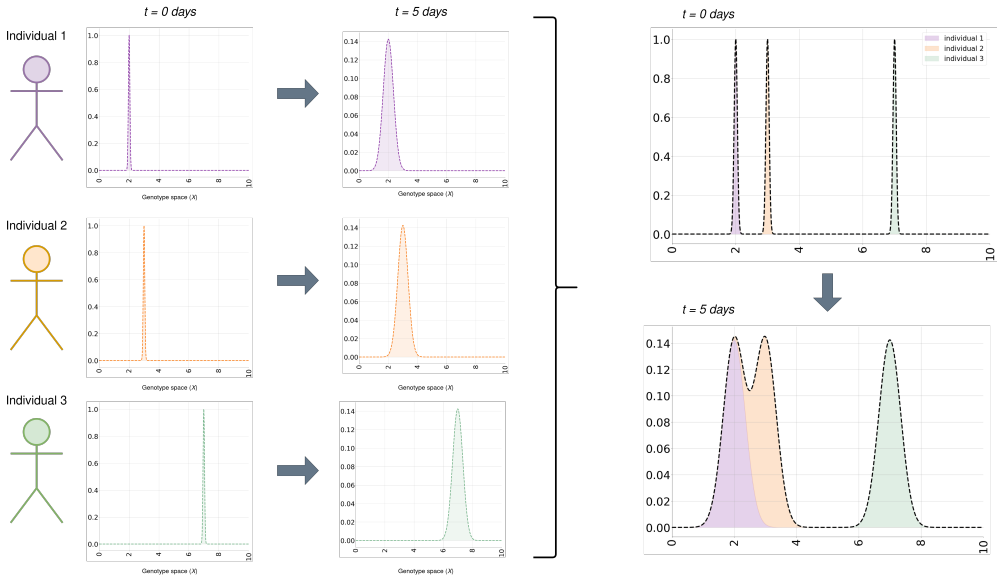

FIGURE 2. A scheme describing the effect of changes in the genotype of individuals due to virus mutations on the genotype of the virus harbored by the population. Three individuals are considered to be initially infected with different strains. Their viral load undergo mutations during five days, which we model as a diffusion process. The distribution of each individual changes accordingly. Since these three processes are independent, the distribution of all infected individuals across the genotype space also undergoes a diffusion process, as shown in the right-hand side of the figure.

To introduce the effect of variant plasticity, we consider a time-dependent diffusion coefficient. It considers that the total number of mutations is proportional to the number of new infections:

$$\theta(t) = \sigma S \int_X \beta(x) \frac{I(x,t)}{1 + K_1 \int_X \phi_x(y, d_0) M(y,t) \mathrm{d}y} \mathrm{d}x$$

The second term on the right-hand side of the equation describes the infection of susceptible cells, which is reduced by the level of population immunity (M). Here, we describe population immunity as the total antibody concentration against a specific strain relative to the total population [24]. It can also be interpreted as the proportion of the population with full protection against the strain, as in another work [50]. The third and fourth terms describe the recovery and mortality of infected cells, respectively. The impact of population immunity is captured by considering that the reduction in susceptibility and severity depend on the broadness of population immunity (d_0), described as follows:

$$\int_X \phi_x(y, d_0) M(y,t) \mathrm{d}y = \begin{cases} \int_X \frac{M(y,t)}{2} \left(1 + \cos\left(\frac{|y-x|}{d_0}\right)\right) & \text{if } |x-y| \leq d_0 \\ 0 \text{ elsewhere} \end{cases}$$

Captured using a radial-basis function to describe the relative efficacy of immunity against strains depending on the genotypic distance between them and the generated antibodies [51]. The third and fourth terms describe the recovery and death of infected individuals, respetively. The rates of recovery and mortality are denoted by μ_1 and μ_2. Note that population immunity also inhibits the mortality of infected individuals with an efficacy equal to K_2. After that, we consider the following equation for recovered individuals, also considered structured

according to the phenotype of the virus by which they were infected:

$$\frac{\partial R}{\partial t}(x,t) = \mu_1 I(x,t) - \delta R(x,t), \tag{2.3}$$

where the first term on the right-hand side of the equation describes the recovery of infected individuals, while the second describes the transition of recovered individuals to the susceptible compartment. In our model, we consider that recovered individuals enjoy a short period of protection and then become susceptible once again [24]. The level of average susceptibility to infections depends on the level of population immunity. To track the number of deaths caused by each variant, we describe the changes in the population of deaths as follows:

$$\frac{\mathrm{d}D}{\mathrm{d}t}(x,t) = \mu_2 \frac{I(x,t)}{1 + K_2 \int_X \phi_x(y,d_0) M(y,t) \mathrm{d}y}. \tag{2.4}$$

Here, the term on the right-hand side of the equation represents the increase in deceased individuals. Finally, we consider the level of population immunity generated through infections, stratified according to the genotype:

$$\frac{\partial M}{\partial t}(x,t) = k \frac{R(x,t)}{N(1 + K \int_X \phi_x(y,d_0) M(y,t) \mathrm{d}y)} - \omega M(x,t), \tag{2.5}$$

where the first term on the right-hand side of the equation describes the increase in population immunity due to recoveries and the second characterizes the loss of immunity due to immune waning, with k and ω representing the rates of immunity increase following recoveries and immune waning, respectively, and N denoting the population size.

2.2. Model calibration and computer implementation

Parameters are varied to study the conditions of variant 1 emergence and the burden associated with it. In the absence of any indications, we consider the default parameters shown in Table 1. The baseline parameters were taken for the case of the initial COVID-19 wave in the United States, although the model can be practically fitted to any other pathogen and area. The infection rate of variant 0 is estimated by fixing the basic reproduction number and recovery rate, and then using the formula to derive variant 0's infection rate. The basic reproduction number is calculated using the next generation matrix method [52, 53], similarly to a previous work [54]

$$\mathcal{R}_0 = \frac{\beta^0 N}{\mu_1 + \mu_2},$$

where N is the size of the population. The simulation is initiated by considering 10 infected individuals with a strain equal to x_0, modelled as a normal distribution with a very small variance equal to 0.02, to account for the relative diversity of strains that consist the initially inhaled virus dose:

$$I(x,0) = \frac{10}{0.02\sqrt{2\pi}} \exp\left(-\frac{1}{2}\frac{-(x-x_0)^2}{0.02^2}\right). \tag{2.6}$$

The numerical implementation of the model is conducted by discretizing the genotype space using a space step of $\mathrm{d}x = 0.1$ G.U. The time step for the simulations is equal to one day ($\mathrm{d}t = 1$ day). The equations are implemented using the Euler-explicit schemes and the diffusion terms are discretized using the second-order central scheme. The code was implemented in the Python programming language. The CPU time for a simulation of 2000 days is estimated at 21 seconds on a computer with an AMD Threadripper processor and 64 GB of RAM. The code is written in a Jupyter notebook and is publicly accessible at the following url: https://github.com/MPS7/Genotype_SIRM.

TABLE 1. Default values for the parameter used in the model. G.U. denotes an arbitrary unit in the genotype space.

Parameter	Value	Calibration method or reference
N	3.2×10^8 (nondimensional)	US population
$\mathcal{R}_0$	3 (nondimensional)	approximate to COVID-19 case
δ	1/10 day^{-1}	[24]
σ	5×10^{-9} $(G.U.)^2/day$	arbitrary
μ_1	$0.985 \times 1/5$ day^{-1}	98.5% CFR and 5 days recovery period
μ_2	$0.015 \times 1/5$ day^{-1}	98.5% CFR and 5 days recovery period
d_0	3 G.U.	arbitrary
K_1	4 (nondimensional)	80% protection against transmission [24]
K_2	18 (nondimensional)	95% protection against death [24]
k	3.18 day^{-1}	fitted such that immunity corresponds to seroprevalence data
K	100 (nondimensional)	[24]
ω	$1/(30 \times 8)$ day^{-1}	Half-life time of immunity is 8 months [55]
adv	0 %	default advantage is 0%
esc	3 (G.U.)	default genomic distance is 3 (G.U.)

3. NUMERICAL EXPERIMENTS

3.1. Broad cross-immunity is necessary for the extinction of previous variants

Our study starts by examining the dynamics of variant emergence and competition under the default parameter set (Table 1). We analyze a fitness landscape comprising two variants with identical transmissibility, separated by a genotypic distance of 3 genomic units (G.U.). We calculate the number of new cases generated by each variant as follows:

$$I^0_{new}(t) = S(t) \int_{x_0-r}^{x_0+r} \beta(x) \frac{I(x,t)}{1 + K_1 \int_X \phi_x(y, d_0) M(y,t) \mathrm{d}y} \mathrm{d}x,$$

$$I^1_{new}(t) = S(t) \int_{x_1-r}^{x_1+r} \beta(x) \frac{I(x,t)}{1 + K_1 \int_X \phi_x(y, d_0) M(y,t) \mathrm{d}y} \mathrm{d}x.$$

Initially, variant 0 triggers an infection wave, peaking around day 110 (see Figure 3A). Subsequently, infection numbers drop until day 150, when waning immunity provokes a resurgence of variant 0. Towards the end of this wave, variant 1 emerges, instigating a new infection wave that peaks at numbers roughly 10% lower than the initial wave. Following this, the two variants enter a phase of alternation, driving successive waves with diminishing impact, attributable to heightened immunity levels. Over 2000 days, these variants collectively account for 10,015,360 infections and 34,990 fatalities. Variant 1 was responsible for 39.69% of the reported infections. Figures 3A–C show the evolution of infections, deaths, and population immunity generated by each of the considered variants. Figure 3D depicts the portion of cases caused by variants 0 and 1. It shows that the two variants alternate in predominance and transition towards co-existing by the end of the simulation time.

Our analysis continues by considering that variant 1 is 50% more transmissible than variant 0. Under this scenario, we observe an alternation in dominance between the two variants. However, when we extend the breadth of cross-immunity to $d_0 = 4$ genomic units (G.U.), the robust immunity elicited by variant 1 impedes the resurgence of variant 0, leading to its extinction. Consequently, variant 1 remains the sole driver of infection and reinfection waves. Cumulatively, these two variants result in 25,092,644 infections and 87,599 deaths, with variant 1 accounting for 89.21% of the total infections. Figures 5A, B, and C illustrate the infection numbers,

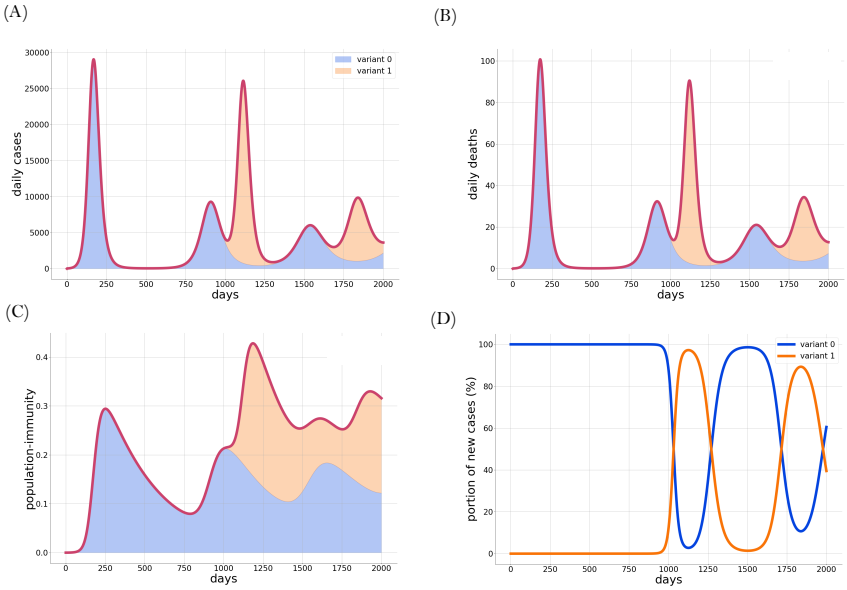

FIGURE 3. Results of numerical experiments showing two alternating variants. These results were obtained by considering the default parameter set. (A) The simulated number of daily infections caused by variants 0 and 1. (B) The number of deaths induced by variants 0 and 1 infections. (C) The level of population immunity against the two variants 0 and 1. (D) The portion of new infections caused by variants 0 and 1, showing an extinction of variant 0.

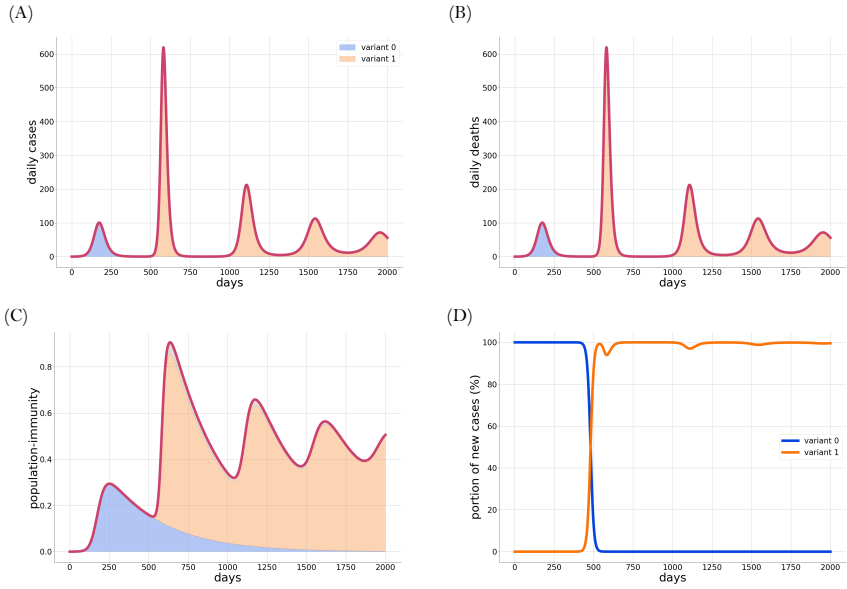

FIGURE 4. Results of numerical simulations when considering that variant 1 has a 50% transmissibility advantage and increasing the breadth of cross-immunity to $d_0 = 4$ G.U. (A) The simulated number of daily infections caused by variants 0 and 1. (B) The number of deaths induced by variants 0 and 1 infections. (C) The level of population immunity against the two variants 0 and 1. (D) The portion of new infections caused by variant 0 and 1, showing an alternation in predominance.

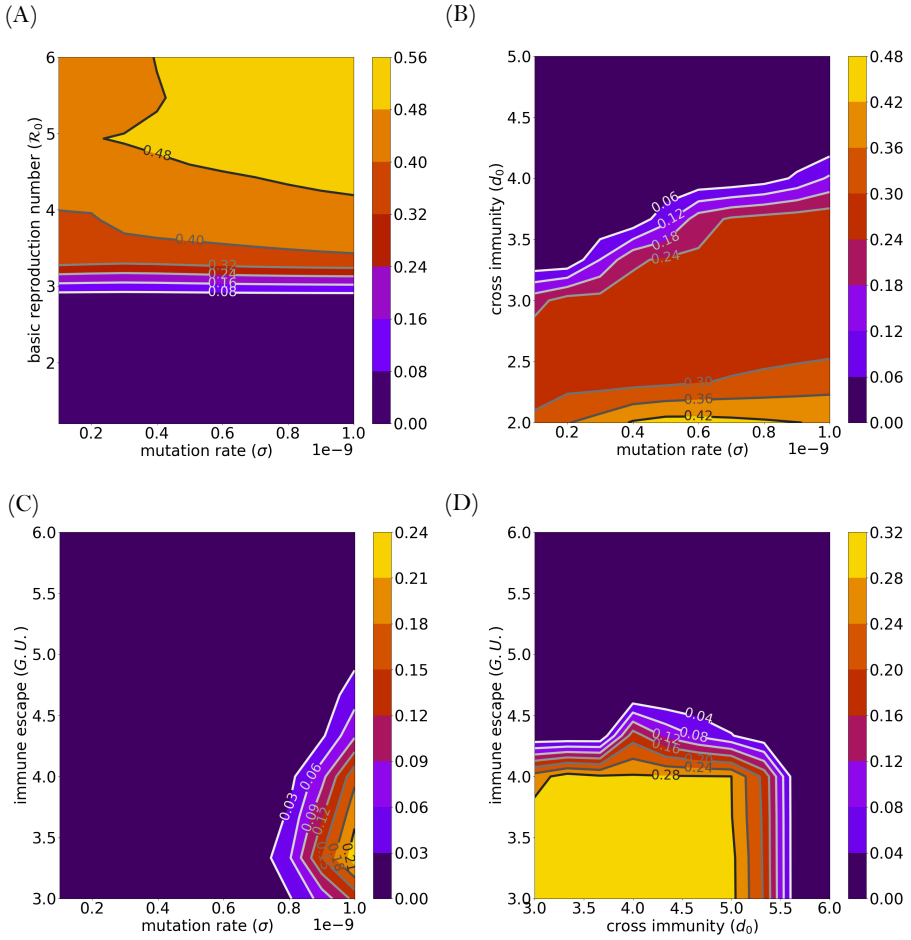

FIGURE 5. The portion of new infections caused by variant 1 when various parameters are varied: (A) the basic reproduction number of variant 0 the mutation rate, (B) the breadth of cross-immunity and the mutation rate, (C) the level of immune escape of variant 1, or genotypic distance separating the two variants, and the mutation rate, and (D) immune escape of variant 1 vs. cross-immunity breadth.

fatalities, and immunity levels associated with each variant, respectively. Figure 5D displays the proportion of infections attributable to each variant.

3.2. Evolutionary and immunological factors driving variant emergence

Leveraging the model's relatively low computational cost, we conducted various numerical experiments to pinpoint the conditions that facilitate variant emergence. These simulations involved changing key parameters related to the virus's epidemiological, evolutionary, and immunological traits. Focusing on the epidemiological aspect, we limited our analysis to the basic reproduction number ($\mathcal{R}_0$) of variant 0. We examined the effects of the mutation rate (σ), the breadth of cross-immunity (d_0), and the genotypic distance separating the two variants ($esc = \Delta x = |x_0 - x_1|$). To estimate the likelihood of variant 1 emerging, we calculated its proportion of total infections using the formula:

$$\sum_n \frac{I^1_{new}(n)}{I_{new}(n)},$$

where $I^1_{new}(n)$ and $I_{new}(n)$ represent the new infections caused by variant 1 and by all strains in day n, respectively.

Figure 5, A illustrates the proportion of infections caused by variant 1 across a range of basic reproduction numbers of variant 0 and mutation rates. Our simulations reveal that a basic reproduction number exceeding 3 is necessary for this variant to emerge. This happens because a higher basic reproduction number increases the rate of infections, leading to more virus replication. The emergence likelihood escalates with higher mutation rates. Specifically, a mutation rate paired with an $\mathcal{R}_0$ greater than 4.5 leads to variant 1 dominating, accounting for over 48% of the infections. Figure 3 demonstrates the impact of cross-immunity breadth (d_0) and mutation rate (σ) on the emergence of variant 1. The results indicate that extensive cross-immunity hinders the emergence of this variant, particularly at lower mutation rates. Higher cross-immunity enables the immunity developed against variant 0 to provide partial protection against variant 1. However, as the mutation rate escalates, the proportion of infections caused by the emerging variant 1 rises, even in the presence of wider cross-immunity.

Figure 5C presents the likelihood of variant 1's emergence under simultaneous changes in its immune escape potential and the virus's overall mutation rate. Immune escape is quantified by the genotypic distance between variants 0 and 1 ($\Delta x = |x_1 - x_0|$). Our simulations reveal that a high level of immune escape leads to lower infection proporitions caused by variant 1, even with a comparatively high mutation rate. This happens because a greater genetic distance between the two variants makes it less likely for the virus to evolve sufficiently to reach variant 1. Figure 5D illustrates the joint influence of immune escape and cross-immunity on the emergence of variant 1, indicating that diminished cross-immunity and a smaller genotypic gap between variants 0 and 1 promote the emergence of variant 1.

3.3. Broad cross-immunity significantly reduces burden and frequency of surges driven by the emergence of highly transmissible variants

We explore the influence of cross-immunity on variant dynamics by conducting simulations that vary both the cross-immunity breadth (d_0) and the relative transmissibility of variant 1. In scenarios where variants exhibit equal transmissibility, an increase in cross-immunity breadth from 2 genomic units (G.U.) delays variant 1's emergence (Figure 6A) and decreases cumulative infection incidents by 32.01%. increasing variant 1's transmissibility reveals that greater cross-immunity reduces the total case incidence by 45.08%, underscoring the critical role robust immunity plays in mitigating the impact of highly transmissible variants. It also reduced the frequency of the incidence of surges as shown in Figure 6B.

In our research, we systematically assess cross-immunity's role in viral variant dynamics by modifying its breadth (d_0) alongside variant 1's transmissibility advantage. Simulations show that when variants have equivalent transmissibility, expanding cross-immunity to 2 genomic units (G.U.) not only postpones the emergence of variant 1, as depicted in Figure 6A but also reduces the overall number of infections by 32.01%. This effect is more pronounced when the transmissibility of variant 1 is increased; in such scenarios, a broader cross-immunity spectrum results in a substantial 45.08% decrease in total case incidence. These findings illuminate the critical influence of robust cross-immunity in controlling the outbreak and spread of highly transmissible viral variants, underscoring its importance in both public health planning and disease mitigation strategies.

3.4. Slower immune waning reduces the burden caused by the emergence of highly transmissible variants

Our study investigates how the speed of immune waning influences the epidemic's trajectory and impact over the 2000-day simulation period. We conduct simulations varying both the immune waning rate (ω) and the transmissibility of variant 1. With rapid immune waning, the number of infections remains elevated post major epidemic surges due to the virus continually infecting individuals with partial protection, as shown in Figure 7, A. Conversely, a slower immune waning rate results in minimal infections following each surge, also impacting surge frequency. Specifically, when immunity's half-life is set at 12 months, only two major surges are observed, in contrast to multiple smaller surges seen with shorter immunity half-lives. This analysis underscores

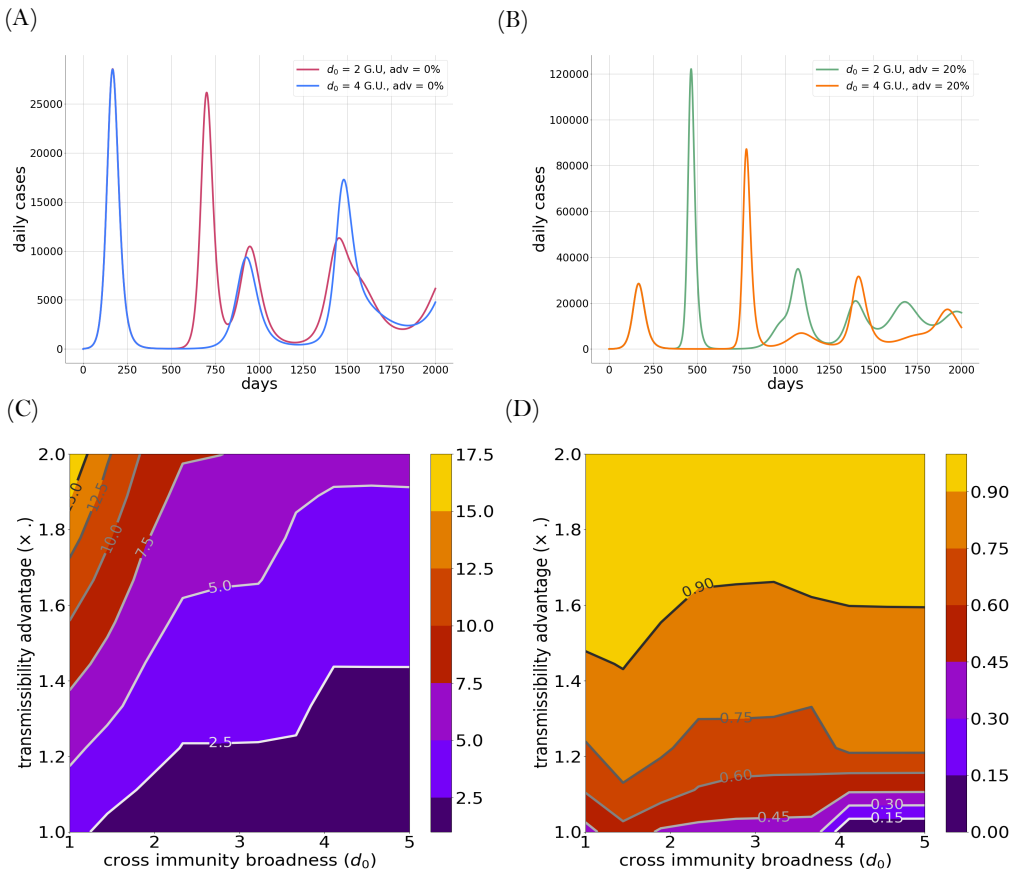

FIGURE 6. The number of daily incident cases in the case where variant 1 has the same transmissibility as variant 0 (A) and when variant 1 has a 20% transmissibility advantage over variant 0. (C) The increase in the cumulative incidence of infections for different values of the cross-immunity broadness and transmissibility advantage relative to the case where $d_0 = 5$ G.U. and $adv = 1\%$. (D) The portion of infections caused by variant 1 for different values of the cross-immunity breadth and variant 1 transmissibility advantage.

the significance of the immune waning rate in determining both the intensity and frequency of infection surges in an epidemic.

Figure 7B illustrates the relative increase in the cumulative burden of infection during a 2000-day period when the half-life time of immune waning and the transmissibility of variant 1 are both varied. It shows that both increasing the speed of immune waning or elevating the transmissibility advantage exacerbate the cumulative number of infections.

4. DISCUSSION

This study introduces a novel infectious disease modeling framework that seamlessly integrates crucial evolutionary and immunological drivers of variant emergence and competition. It incorporates elements contributing to virus evolution, such as the mutation rate, as well as mechanisms regulating the efficacy of population immunity, such as cross-immunity, immune waning, and immunity-specific efficacy. Our framework can be easily calibrated to incorporate the epidemiological, immunological, and evolutionary dynamics of any pathogen.

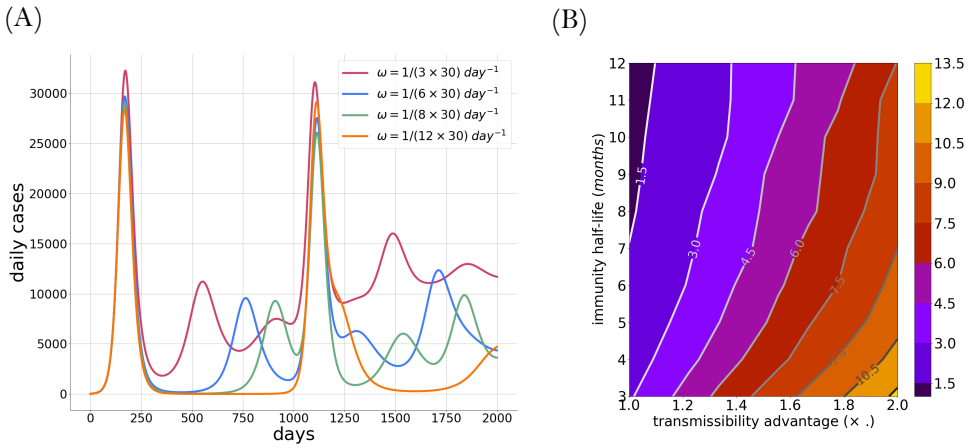

FIGURE 7. (A) The daily number of new infections for different immune waning rate values. (B) The relative increase in the number of infections compared to the case where the half-life time of immunity is 12 months and the transmissibility advantage of 1.

After calibrating the model, we reveal two primary patterns in variant dynamics, depending on the cross-immunity levels and the transmissibility of emerging variants. In scenarios where the emergent variant is similar to the original in transmissibility, a pattern of alternating dominance is observed, similar to seasonal respiratory viruses like influenza and RSV. The incorporation of additional parameters, such as viral frequency and seasonal fluctuations, could synchronize these alternating cycles with seasonal changes, enabling the climate-driven resonance observed in influenza variant alternations [56].

Increasing the transmissibility of variant 1 and cross-immunity breadth in our model shows variant 1 becoming dominant, preventing variant 0's resurgence. In such scenarios, the rise of variant 1 drives new infection waves as immunity levels wane, similar to SARS-CoV-2 dynamics where fitter variants eclipse their predecessors. Our findings indicate that these dynamics occur with high cross-immunity breadth, as the strong immunity from the dominant variant effectively prevents the re-emergence of its predecessor. Hence, selective pressure from immunity is necessary for the extinction of the less aggressive variant. These results agree with the pathogen invasion theory (PIT) developed using a different modeling framework [57].

In our numerical experiments, we have explored the conditions that lead to the emergence of new variants, focusing on the virus's evolutionary potential, immune-driven selective pressure, and characteristics of emerging variants. Our simulations reveal that a high basic reproduction number is essential for variants to emerge, even with higher mutation rates, as fewer infections mean fewer opportunities for viral replication and mutation. These findings agree with the dynamics of variant emergence in COVID-19. Indeed, the emergence of highly transmissibile variants and their predominance has accelerated the rate by which the virus evolves, leading to more frequent emergence of variants. Thus, reducing infection rates through non-pharmaceutical measures could diminish variant emergence chances. Additionally, our results suggest that broad cross-immunity lowers variant emergence chances. We can specualte that the development of cocktail vaccines that offer protection against multiple strains will minimize the chances of variant emergence. Further, we have shown that immune escaping variants are less likely to emerge, especially when the mutation rate is lower or the cross-immunity is higher.

We explored how immunity characteristics impact the burden of variant emergence. Our simulations revealed that enhanced cross-immunity significantly lowers the frequency and severity of infection waves, particularly when a variant has a transmissibility advantage. Slowing down the rate of immune waning also impacted wave frequency and reduced infections between waves. These findings underscore the importance of developing vaccines that provide broad, long-lasting protection to effectively manage the burden of emergent viral variants.

Our research acknowledges certain limitations. Firstly, we model genetic drift in infected populations as following a diffusion process, where the genetic drift caused by each mutation is considered to be sampled

from a normal distribution, in agreement with several previous theoretical studies [36–38] but differing from others that use distributions like the log-normal [58]. This choice allows the derivation of a system of reaction-diffusion equations, which describes the population-level changes in the genotype. Secondly, our model's fitness landscape is simplified to two variants separated by genetic distance, which may not fully capture the complexity of RNA virus evolution that includes multiple strains and clades. This simplification is due to our focus on the theoretical analysis of virus emergence, competition, and extinction, rather than specific diseases. Extensions to more complex models or including actual antigenic maps for variants are possible for specific diseases [59]. Lastly, we do not account for mobility and climate effects on variant dynamics. These areas were explored in other studies through the modulation of the infection rate [60–62], as well as in our recent adaptation of the model to study influenza co-circulation dynamics [49]. Finally, we focused exclusively on the effect of symmetrical cross-immunity in this study. The impact of asymmetrical cross-immunity can be explored by modifying the formula used in the radial basis function in $\phi_x(y, d_0)$. Asymmetrical cross-immunity can provide a survival advantage to certain variants, enabling them to outcompete others. The above-mentioned limitations were considered allow the interpretation of the model's prediction and to derive general insights which can be applied to a wide range of diseases. In forthcoming studies, we will use the current model to explore formulations for multivalent vaccines that are most effective against each type of variant.

Data availability statement

The code used in this paper is available online in a Github repository: https://github.com/MPS7/Genotype_SIRM [63].

References

[1] J.K. Miller, K. Elenberg and A. Dubrawski, Forecasting emergence of covid-19 variants of concern. *PLoS One* **17** (2022) e0264198.

[2] P. Gupta, V. Gupta, C.M. Singh and L. Singhal, Emergence of covid-19 variants: an update. *Cureus* **15** (2023).

[3] W. Tong, F. Liu, H. Zheng, C. Liang, Y.-j. Zhou, Y.-f. Jiang, T.-l. Shan, F. Gao, G.-x. Li and G.-z. Tong, Emergence of a pseudorabies virus variant with increased virulence to piglets. *Vet. Microbiol.* **181** (2015) 236–240.

[4] A.M. Carabelli, T.P. Peacock, L.G. Thorne, W.T. Harvey, J. Hughes, S.J. Peacock, W.S. Barclay, T.I. De Silva, G.J. Towers and D.L. Robertson, Sars-cov-2 variant biology: immune escape, transmission and fitness. *Nat. Rev. Microbiol.* **21** (2023) 162–177.

[5] A.M. Carabelli, T.P. Peacock, L.G. Thorne, W.T. Harvey, J. Hughes, C.-G.U.C. de Silva Thushan, S.J. Peacock, W.S. Barclay, T.I. de Silva, G.J. Towers, *et al.*, SARS-Cov-2 variant biology: immune escape, transmission and fitness. *Nat. Rev. Microbiol.* **21** (2023) 162–177.

[6] C.W. Tan, W.N. Chia, F. Zhu, B.E. Young, N. Chantasrisawad, S.-H. Hwa, A.Y.-Y. Yeoh, B.L. Lim, W.C. Yap, S.K.M. Pada, *et al.*, SARS-Cov-2 omicron variant emerged under immune selection. *Nat. Microbiol.* **7** (2022) 1756–1761.

[7] S. François, S. Nazki, S. Vickers, H. Fournié, C.M., Perrins, A.J., Broadbent, O.G. Pybus and S.C. Hill. Genetic diversity, recombination and cross-species transmission of a waterbird gammacoronavirus in the wild. *J. Gen. Viro.*, **104** (2023) 001883.

[8] R.N. Thompson, E. Southall, Y. Daon, F.A. Lovell-Read, S. Iwami, C.P. Thompson and U. Obolski, The impact of cross-reactive immunity on the emergence of sars-cov-2 variants. *Front. Immunol.* **13** (2023) 1049458.

[9] A. Vié, Emergence of more contagious covid-19 variants from the interaction of viruses and policy interventions, in *Artificial Life Conference Proceedings 33*, Vol. 2021. MIT Press, Cambridge, MA, USA (2021) 15.

[10] F. Brauer, P. Van den Driessche, J. Wu and L.J. Allen, Mathematical Epidemiology, Vol. 1945. Springer (2008).

[11] R. Saxena, M. Jadeja and V. Bhateja, *Exploring Susceptible-Infectious-Recovered (SIR) Model for COVID-19 Investigation*. Springer (2022).

[12] V. Volpert, M. Banerjee and S. Petrovskii, On a quarantine model of coronavirus infection and data analysis. *Math. Model. Natural Phenomena* **15** (2020) 24.

[13] H. Andersson and T. Britton, Stochastic Epidemic Models and Their Statistical Analysis, Vol. 151. Springer Science & Business Media (2012).

[14] J.P. Medlock, *The Effect of Stochastic Migration on an SIR Model for the Transmission of HIV*. PhD thesis, School of Mathematics, Georgia Institute of Technology (1999).

[15] M. Lu, X.-y. Zheng, W.-n. Jia and C.-z. Tian, Analysis and prediction of improved SEIR transmission dynamics model: taking the second outbreak of COVID-19 in Italy as an example. *Front. Public Health* **11** (2023).

[16] X. Weng, Q. Chen, T.K. Sathapathi, X. Yin and L. Wang, Impact of school operating scenarios on COVID-19 transmission under vaccination in the us: an agent-based simulation model. *Sci. Rep.* **13** (2023) 12836.

[17] A. Bouchnita and A. Jebrane, A hybrid multi-scale model of covid-19 transmission dynamics to assess the potential of non-pharmaceutical interventions. *Chaos Solitons Fractals* **138** (2020) 109941.

[18] A.E.S. Almocera and E.A. Hernandez-Vargas, Coupling multiscale within-host dynamics and between-host transmission with recovery (sir) dynamics. *Math. Biosci.* **309** (2019) 34–41.

[19] A.E.S. Almocera, V.K. Nguyen and E.A. Hernandez-Vargas, Multiscale model within-host and between-host for viral infectious diseases. *J. Math. Biol.* **77** (2018) 1035–1057.

[20] J.W. Doran, R.N. Thompson, C.A. Yates and R. Bowness, Mathematical methods for scaling from within-host to population-scale in infectious disease systems. *Epidemics*, **45** (2023) 100724.

[21] M.O. Adewole, T.S. Faniran, F.A. Abdullah and M.K. Ali, COVID-19 dynamics and immune response: linking within-host and between-host dynamics. *Chaos Solitons Fractals* **173** (2023) 113722.

[22] S. Ghosh, M. Banerjee and V. Volpert, Immuno-epidemiological model-based prediction of further covid-19 epidemic outbreaks due to immunity waning. *Math. Model. Natural Phenomena* **17** (2022) 9.

[23] M. Saade, S. Ghosh, M. Banerjee and V. Volpert, Delay epidemic models determined by latency, infection, and immunity duration. *Math. Biosci.* (2024) 109155.

[24] A. Bouchnita, K. Bi, S.J. Fox and L.A. Meyers, Projecting omicron scenarios in the us while tracking population-level immunity. *Epidemics*, **46** (2024) 100746.

[25] O. Khyar and K. Allali, Global dynamics of a multi-strain SEIR epidemic model with general incidence rates: application to covid-19 pandemic. *Nonlinear Dyn.* **102** (2020) 489–509.

[26] K. Koelle, S. Cobey, B. Grenfell and M. Pascual, Epochal evolution shapes the phylodynamics of interpandemic influenza a (h3n2) in humans. *Science* **314** (2006) 1898–1903.

[27] M. Massard, R. Eftimie, A. Perasso and B. Saussereau, A multi-strain epidemic model for covid-19 with infected and asymptomatic cases: application to French data. *J. Theor. Biol.* **545** (2022) 111117.

[28] K.W. Okamoto, V. Ong, R. Wallace, R. Wallace and L.F. Chaves, When might host heterogeneity drive the evolution of asymptomatic, pandemic coronaviruses? *Nonlinear Dyn.* **111** (2023) 927–949.

[29] M. Łuksza and M. Lässig, A predictive fitness model for influenza. *Nature* **507** (2014) 57–61.

[30] F. Fabre, J. Montarry, J. Coville, R. Senoussi, V. Simon and B. Moury, Modelling the evolutionary dynamics of viruses within their hosts: a case study using high-throughput sequencing. *PLoS Pathogens* **8** (2012) e1002654.

[31] B.T. Grenfell, O.G. Pybus, J.R. Gog, J.L. Wood, J.M. Daly, J.A. Mumford and E.C. Holmes, Unifying the epidemiological and evolutionary dynamics of pathogens. *Science* **303** (2004) 327–332.

[32] C.M. Saad-Roy, C.J.E. Metcalf and B.T. Grenfell, Immuno-epidemiology and the predictability of viral evolution. *Science* **376** (2022) 1161–1162.

[33] E.M. Volz, K. Koelle and T. Bedford, Viral phylodynamics. *PLoS Computat. Biol.* **9** (2013) e1002947.

[34] S. Gupta, N. Ferguson and R. Anderson, Chaos, persistence, and evolution of strain structure in antigenically diverse infectious agents. *Science* **280** (1998) 912–915.

[35] N.M. Ferguson, A.P. Galvani and R.M. Bush, Ecological and immunological determinants of influenza evolution. *Nature* **422** (2003) 428–433.

[36] N. Bessonov, G. Bocharov, A. Meyerhans, V. Popov and V. Volpert, Existence and dynamics of strains in a nonlocal reaction-diffusion model of viral evolution. *SIAM J. Appl. Math.* **81** (2021) 107–128.

[37] N. Bessonov, D. Neverova, V. Popov and V. Volpert, Emergence and competition of virus variants in respiratory viral infections. *Front. Immunol.* **13** (2022).

[38] M. Banerjee, T. Lipniacki, A. d'Onofrio and V. Volpert, Epidemic model with strain-dependent transmission rate. *Commun. Nonlinear Sci. Numer. Simul.* **114** (2022) 106641.

[39] N. Bessonov, N. Reinberg, M. Banerjee and V. Volpert, The origin of species by means of mathematical modelling. *Acta Biotheor.* **66** (2018) 333–344.

[40] A. Bouchnita, Genotype-structured modeling of variant emergence and its impact on virus infection. *Mathematics* **13** (2025) 167.

[41] A. Bouchnita and V. Volpert, Phenotype-structured model of intra-clonal heterogeneity and drug resistance in multiple myeloma. *J. Theor. Biol.* **576** (2024) 111652.

[42] R.E. Stace, T. Stiehl, M.A. Chaplain, A. Marciniak-Czochra and T. Lorenzi, Discrete and continuum phenotype-structured models for the evolution of cancer cell populations under chemotherapy. *Math. Model. Natural Phenomena* **15** (2020) 14.

[43] K. Koelle, M.A. Martin, R. Antia, B. Lopman and N.E. Dean, The changing epidemiology of SARS-Cov-2. *Science* **375** (2022) 1116–1121.

[44] J.S. Lavine, O.N. Bjornstad and R. Antia, Immunological characteristics govern the transition of COVID-19 to endemicity. *Science* **371** (2021) 741–745.

[45] E. Howerton, L. Contamin, L.C. Mullany, M. Qin, N.G. Reich, S. Bents, R.K. Borchering, S.-m. Jung, S.L. Loo, C.P. Smith, *et al.* Evaluation of the us COVID-19 scenario modeling hub for informing pandemic response under uncertainty. *Nat. Commun.* **14** (2023) 7260.

[46] L. Meyers, K. Bi, S. Bandekar, A. Bouchnita and S. Fox, Scenario projections for SARS-Cov-2, influenza, and RSV burden in the us, **41** (2023–2024). 2023.

[47] F. Owusu-Dampare and A. Bouchnita, Equitable bivalent booster allocation strategies against emerging SARS-Cov-2 variants in us cities with large Hispanic communities: the case of El Paso county, Texas. *Infect. Dis. Model.* **8** (2023) 912–919.

[48] M. Łuksza and M. Lässig, A predictive fitness model for influenza. *Nature* **507** (2014) 57–61.

[49] A. Bouchnita and B. Djafari-Rouhani, Integrating genomic, climatic, and immunological factors to analyze seasonal patterns of influenza variants. *Symmetry* **16** (2024) 943.

[50] S.E. Morris, V.E. Pitzer, C. Viboud, C.J.E. Metcalf, O.N. Bjørnstad and B.T. Grenfell, Demographic buffering: titrating the effects of birth rate and imperfect immunity on epidemic dynamics. *J. Roy. Soc. Interface* **12** (2015) 20141245.

[51] G. Luo, Z. Yang, C. Zhan and Q. Zhang, Identification of nonlinear dynamical system based on raised-cosine radial basis function neural networks. *Neural Process. Lett.* **53** (2021) 355–374.

[52] O. Diekmann, J.A.P. Heesterbeek and J.A.J. Metz, On the definition and the computation of the basic reproduction ratio r 0 in models for infectious diseases in heterogeneous populations. *J. Math. Biol.* **28** (1990) 365–382.

[53] P. Van den Driessche and J. Watmough, Reproduction numbers and sub-threshold endemic equilibria for compartmental models of disease transmission. *Math. Biosci.* **180** (2002) 29–48.

[54] S.R. Bandekar and M. Ghosh, Mathematical modeling of COVID-19 in India and its states with optimal control. *Model. Earth Syst. Environ.* **8** (2022) 2019–2034.

[55] K.E. Clarke, J.M. Jones, Y. Deng, E. Nycz, A. Lee, R. Iachan, A.V. Gundlapalli, A.J. Hall and A. MacNeil, Seroprevalence of infection-induced SARS-Cov-2 antibodies—united states, September 2021–February 2022. *Morbid. Mortal. Wkly Rep.* **71** (2022) 606.

[56] E. Lofgren, N.H. Fefferman, Y.N. Naumov, J. Gorski and E.N. Naumova, Influenza seasonality: underlying causes and modeling theories. *J. Virol.* **81** (2007) 5429–5436.

[57] S.W. Park, S. Cobey, C.J.E. Metcalf, J.M. Levine and B.T. Grenfell, Predicting pathogen mutual invasibility and co-circulation. *Science* **386** (2024) 175–179.

[58] A. Kousathanas and P.D. Keightley, A comparison of models to infer the distribution of fitness effects of new mutations. *Genetics* **193** (2013) 1197–1208.

[59] D.J. Smith, A.S. Lapedes, J.C. De Jong, T.M. Bestebroer, G.F. Rimmelzwaan, A.D. Osterhaus and R.A. Fouchier, Mapping the antigenic and genetic evolution of influenza virus. *Science* **305** (2004) 371–376.

[60] A. d'Onofrio and P. Manfredi, Behavioral sir models with incidence-based social-distancing. *Chaos Solitons Fractals* **159** (2022) 112072.

[61] S.J. Fox, M. Lachmann, M. Tec, R. Pasco, S. Woody, Z. Du, X. Wang, T.A. Ingle, E. Javan, M. Dahan, *et al.*, Real-time pandemic surveillance using hospital admissions and mobility data. *PNAS* **119** (2022) e2111870119.

[62] P. Shi, Y. Dong, H. Yan, C. Zhao, X. Li, W. Liu, M. He, S. Tang and S. Xi, Impact of temperature on the dynamics of the covid-19 outbreak in china. *Sci. Total Environ.* **728** (2020) 138890.

[63] A. Bouchnita, S. R. Bandekar, K. Bi, S. J. Fox, and J. Garcia, The interplay between evolutionary and immunological dynamics regulates virus variant emergence and competition. *Mathematical Modelling of Natural Phenomena* https://doi.org/10.1051/mmnp/2025006 (2025).